Impact of Body Mass Index on Power Distribution in High-Power RF Ablation for Atrial Fibrillation

Minha Anees[1], Zoraida Moreno Weidmann[2], David Vilades Medel[2], Jose M Guerra[2], Luca Gerardo-Giorda[1,3], Argyrios Petras[1]

[1] Johann Radon Institute for Computational and Applied Mathematics (RICAM), Austrian Academy of Sciences, Linz, Austria
[2] Department of Cardiology, Hospital de la Santa Creu i Sant Pau, IIB Sant Pau, Universitat Autònoma de Barcelona, CIBER CV, Barcelona, Spain
[3] Institute for Mathematical Methods in Medicine and Data-Based Modelling, Johannes Kepler University, Linz, Austria

Abstract

Atrial fibrillation (AF) is the most common cardiac arrhythmia, with obesity identified as a significant risk factor. Pulmonary vein isolation (PVI) via radiofrequency ablation (RFA) is a key treatment for AF, though higher BMI is associated with increased recurrence rates. This study aims to investigate how obesity influences energy dispersion within torso geometries. To this end, we developed three virtual patient models (normal, pre obese, and morbidly obese) to analyze BMI impact on the power distribution during RFA. Our results demonstrate significant variations in tissue power distribution and baseline impedances across BMI categories, highlighting the need for tailored ablation strategies in obese patients to enhance treatment efficacy. Incorporating BMI related variations in RFA energy delivery can help guide personalized AF ablations, potentially improving clinical outcomes.

1. Introduction

AF is the most prevalent cardiac arrhythmia, leading to increased morbidity, mortality, and reduced quality of life. According to the World Health Organization (WHO), obesity (BMI $> 30\,\mathrm{kg/m^2}$) [1] is a major risk factor for AF. Population-based studies have shown that obese individuals have a 49% higher risk of developing AF compared to those with normal weight [2], and this risk increases proportionally with rising BMI.

Pulmonary vein isolation (PVI) is a common ablation procedure used to treat AF and can be performed using high-power, short-duration (HPSD) RFA. Compared with conventional ablation protocols, the HPSD approach has been associated with shorter procedure times and improved clinical outcomes [3]. However, patient obesity can significantly influence the effectiveness of ablation procedures. Clinical studies have demonstrated a clear relationship between higher BMI and increased rates of AF recurrence following ablation. For example, post-ablation recurrence at 12 months was reported as 35.2% in normal-weight patients, 35.7% in pre-obese, 43.6% in obese, and 48.0% in morbidly obese patients [4]. Although AF ablation remains generally safe across all BMI categories, morbid obesity has been linked to reduced procedural success [5], underscoring the importance of considering BMI in treatment planning.

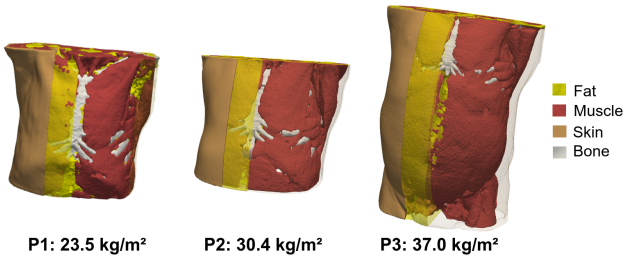


Figure 1. The virtual patient models show muscle, fat, and skin compositions with different BMI across three virtual patients.

Computer simulations of the procedure can aid in the understanding of the underlying mechanisms that lead to the reduction of the efficacy for patients with high BMI. In this study, we developed three 3D virtual patient models representing different BMI groups. For each virtual patient, we assessed (as a proxy for temperature variations [6]) the power distribution resulting from typical ablation sites in AF treatments, aiming to determine how obesity influences energy dispersion within torso geometries.

2. Methods

2.1. Study design

We developed 3D in-silico models of three virtual male patients, each representing a different BMI category: normal (23.5 kg/m^2), pre-obese (30.4 kg/m^2), and morbidly obese (37.0 kg/m^2). To ensure relevance to real clinical scenarios, all virtual patients were modeled using CT scan data from individuals over 50 years of age. This age group is more commonly affected by AF and related cardiovascular conditions.

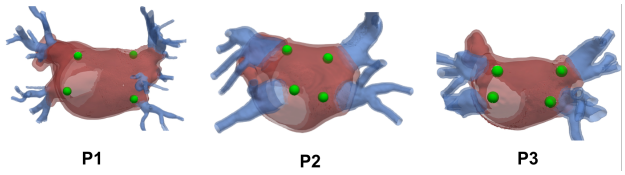


Figure 2. Electrode positions at the left posterior wall near the pulmonary veins for each of the three virtual patients.

2.2. Geometry

The 3D virtual patient models were constructed from thoracic CT scans using 3D Slicer software [7]. The segmentation included major body compartments such as the heart, lungs, liver, adipose tissue, and muscles, along with other organs and tissues, as illustrated in Figure 1. We discretized the multilabel segmentation into an unstructured tetrahedral mesh using Meshtool [8]. The catheter and electrode body were designed with Salome software [9]. The catheter was introduced via the inferior vena cava, advanced across the interatrial septum, and positioned against the left atrial wall. The tip electrode, featuring a spherical design as described in [6], was inserted 0.5 mm into different tissue locations, shown in Figure 2.

2.3. Mathematical model

We solved the electrical potential equation for the torso geometries

$$-\nabla \cdot \sigma \nabla \phi = 0,$$

where σ is the electrical conductivity, and ϕ is the electrical potential. A potential V_0 is applied at the upper boundary of the electrode, as in [6], while zero voltage condition is imposed on the dispersive patch (DP) to close the circuit. The remaining boundaries considered electrically isolated. We used the methodology described in [6] to assess power dissipation within the left atrial tissue.

2.4. Model parameters

The model parameters are obtained from a publicly available database [10], with different tissue types measured at a frequency of 500 kHz. We used the electrical conductivity values of the porcine pericardium [11] to model human pericardial conductivity, as no corresponding human values are available in the literature.

Table 1. Electrical conductivity of the different tissues within the virtual patients torsos.

Parameters	**Conductivity (S/m)**
Bone	0.02
Lungs	0.12
Liver	0.14
Stomach	0.55
Esophagus (lumen)	10^{-5}
Esophagus	0.55
Spleen	0.14
Electrode	4.6×10^6
Cardiac Tissue	0.28
Pericardium	0.17
Blood	0.74
Blood Vessel Wall	0.32
Kidney	0.22
Pancreas	0.56
Prostate	0.4
Small intestine	0.72
Colon	0.27
Gallbladder	0.9
Urinary Bladder Wall	0.2
Fat	0.02
Muscle	0.45
Skin	0.15

2.5. Ablation protocol

Four electrode positions were selected on the posterior LA wall, near the pulmonary veins, commonly targeted in PVI procedures: Left Superior Pulmonary Vein (LSPV), Right Superior Pulmonary Vein (RSPV), Left Inferior Pulmonary Vein (LIPV), and Right Inferior Pulmonary Vein (RIPV) as shown in Figure 2. Additionally, we placed horizontally the dispersive patch at the center of the back of the torso, corresponding to hPC position in [6], and simulated a high-power setting of 90 W.

3. Results

A total of 12 simulations (4 ablations for each of the 3 patients) were performed using our in-house developed

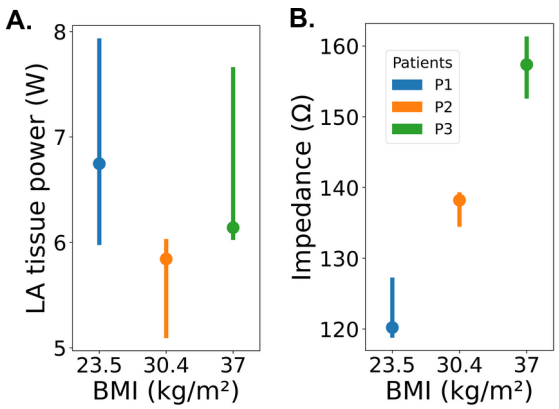


Figure 3. The baseline impedance (**A**) and the power dissipated in the left atrial tissue (**B**) across all BMI categories. The vertical lines represent the range of values for each BMI category, and the markers indicate the median.

AblaFEMx library, which is built on the open-source FEniCSx software. An open access version can be found in https://linzlabinsilmed.github.io/.

First, we explored the relationship between BMI and **baseline** impedance. The values ranged between 118 and 129 Ω for a normal weight patient (P1), 134 and 139 Ω for a pre-obese patient (P2) and 157 and 161 Ω for a morbidly obese patient (P3). This indicates that as BMI increases, impedance also increases, suggesting a direct relationship between the two, shown in Figure 3 (A).

On the contrary, no strong or direct correlation between BMI and power dissipated in the left atrial (LA) tissue is observed, as the values fluctuate without a clear pattern in Figure 3 (B). P1 exhibits the highest median LA tissue power dissipation at approximately 6.8 W with a large range, indicating significant variability. In contrast, P2 demonstrates the lowest median LA tissue power dissipation, around 5.9 W, with the smallest variability, suggesting more consistent values within this group. P3 shows slightly higher median tissue power dissipation than P2, approximately 6.2 W, but remains lower than P1. The ranges for P1 and P3 suggest greater variability in these groups, indicating that factors beyond BMI, such as differences in cardiac anatomy, may influence LA tissue power dissipation.

In relation to the wall thickness, the tissue power dissipation clearly increases for thicker walls, for each patient individually (see Figure 4 A). However, at the same wall thickness, the tissue power dissipation is lower for the obese patients compared to the normal weight one, showing that BMI plays a significant role in the power dissipation - wall thickness relationship.

Further investigating the tissue power dissipation per vein, P1 showed comparable or higher power dissipation compared to other patients, as in Figure 4 B. The highest

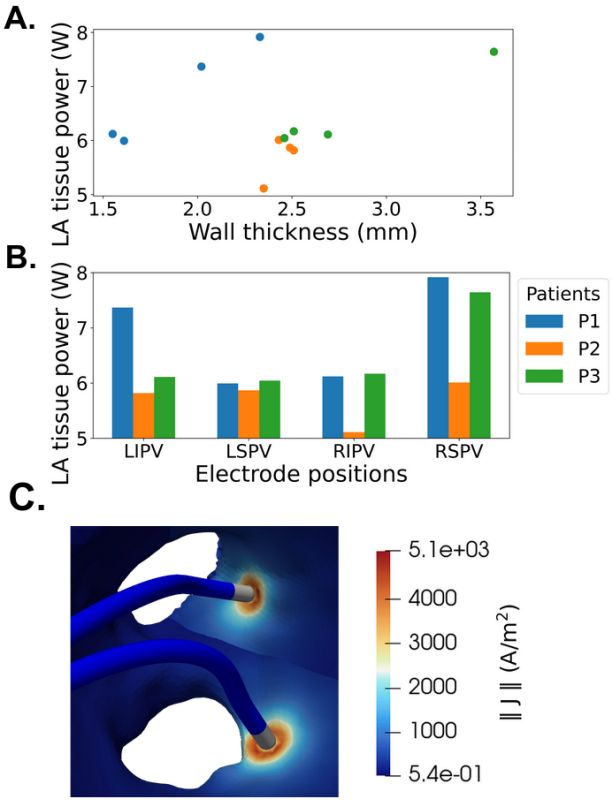


Figure 4. Power dissipation in LA tissue in relation to wall thickness (**A**) and the pulmonary vein location (**B**) at each electrode position. **C**. Current density (**J**) in P3 shown at the RSPV (upper vein) and the RIPV (lower vein).

power dissipation for each patient among the 4 pulmonary veins is dissipated near RSPV. As shown in Figure 4C, despite similar current density distributions at both ablation sites, higher power dissipation is observed at RSPV (top electrode position) compared to LIPV (bottom electrode position). Near the LSPV, all BMI categories exhibited similar power dissipation, indicating that certain anatomical sites may be less influenced by BMI-related variations. In RIPV, the power dissipated at electrode positions P1 and P3 is the same, whereas P2 shows the least power dissipation.

4. Discussion

We present the first computational study that provides insights in the relation of BMI and power distribution in RFA using anatomically detailed virtual patients that include the body fat and muscle. Our findings highlight a clear relationship between BMI and baseline impedance, reinforcing the idea that body composition plays a significant role in ablation, as observed from clinical ablation procedures [4].

While no direct correlation of BMI and tissue power is observed, correlation of the dissipated power and pulmonary vein is observed. Such discrepancy has also been observed clinically [12], with fewer reconnections in posterior RSPV, and most reconnections near posterior RIPV.

Furthermore, a clear correlation of the wall thickness and the dissipated tissue power is observed, which is altered for obese patients. Clinical studies have focused on tailoring ablation power on the wall thickness [13]. However, at present, there are no established guidelines that specifically address variations in impedance related to BMI during ablation.

A limitation of this study is the variation in torso length across BMI groups, which may have influenced energy dissipation patterns; this aspect is the focus of ongoing work. In addition, differences in cardiac tissue composition may significantly affect PVI outcomes, an aspect not accounted for in this study.

5. Conclusions

Our study demonstrates a clear positive correlation between BMI and impedance, with higher impedance values observed as BMI increases. No strong direct relationship was found between BMI and LA tissue power dissipation, though normal BMI patients exhibited higher left atrial tissue power dissipation compared to others. Ablation sites near RSPV showed the highest dissipation across all BMI categories. More power is dissipated in thicker tissues per patient, with obese patients exhibiting significantly lower power at the same tissue thickness as normal weight ones.

Acknowledgments

A.P and L.GG acknowledge the partial support of the State of Upper Austria. The research was funded in part by the Austrian Science Fund (FWF) P35374N. For the purpose of Open Access, the author has applied a CC-BY public copyright licence to any Author Accepted Manuscript (AAM) version arising from this submission.

References

[1] Consultation W. Obesity: preventing and managing the global epidemic. World Health Organization Technical Report Series 2000;894:1–253.

[2] Liu F, Song T, Hu Q, Zhu X, Zhao H, Tan Z, Yu P, Ma J, Luo J, Liu X. Body mass index and atrial fibrillation recurrence post ablation: A systematic review and dose-response meta-analysis. Frontiers in Cardiovascular Medicine 2023; 9:999845.

[3] Kotadia ID, Williams SE, O'Neill M. High-power, short-duration radiofrequency ablation for the treatment of af. Arrhythmia Electrophysiology Review 2019;8(4):265.

[4] Providencia R, Adragão P, de Asmundis C, Chun J, Chierchia G, Defaye P, Anselme F, Creta A, Lambiase PD, Schmidt B, et al. Impact of body mass index on the outcomes of catheter ablation of atrial fibrillation: a european observational multicenter study. Journal of the American Heart Association 2019;8(20):e012253.

[5] Tabaja C, Younis A, Santageli P, Farwati M, Braghieri L, Nakagawa H, Saliba WI, Madden R, Bouscher P, Kanj M, et al. Impact of obesity on catheter ablation of atrial fibrillation: patient characteristics, procedural complications, outcomes, and quality of life. Journal of Cardiovascular Electrophysiology 2023;34(8):1648–1657.

[6] Anees M, Moreno Weidmann Z, Viladés Medel D, Guerra JM, Gerardo-Giorda L, Petras A. Impact of the dispersive patch placement on dissipated power in radiofrequency ablation for pulmonary vein isolation via a virtual patient study. Scientific Reports 2025;15(1):6986.

[7] Fedorov A, Beichel R, Kalpathy-Cramer J, Finet J, Fillion-Robin JC, Pujol S, Bauer C, Jennings D, Fennessy F, Sonka M, Buatti J, Aylward SR, Miller JV, Pieper S, Kikinis R. 3d slicer as an image computing platform for the quantitative imaging network. Magnetic Resonance Imaging 2012; 30(9):1323–1341.

[8] Neic A, Gsell MA, Karabelas E, Prassl AJ, Plank G. Automating image-based mesh generation and manipulation tasks in cardiac modeling workflows using meshtool. SoftwareX 2020;11:100454.

[9] CEA and EDF (SALOME Platform). Salome: The open-source integration platform for numerical simulation, 2025. URL https://www.salome-platform.org/.

[10] Hasgall P, Di Gennaro F, Baumgartner C, Neufeld E, Lloyd B, Gosselin M, Payne D, Klingenböck A, Kuster N. IT'IS Database for thermal and electromagnetic parameters of biological tissues, 2022. URL itis.swiss/database.

[11] National Institute of Information and Communications Technology (NICT). Database of tissue dielectric properties for electromagnetic modeling of human body. Online. URL https://www2.nict.go.jp/cgi-bin/202303080003/public_html/index.py/.

[12] Kueffer T, Bordignon S, Neven K, Blaauw Y, Hansen J, Adelino R, Ouss A, Füting A, Roten L, Mulder BA, et al. Durability of pulmonary vein isolation using pulsed-field ablation: results from the multicenter eu-poria registry. Clinical Electrophysiology 2024;10(4):698–708.

[13] Falasconi G, Penela D, Soto-Iglesias D, Francia P, Saglietto A, Turturiello D, Viveros D, Bellido A, Alderete J, Zaraket F, et al. Personalized pulmonary vein isolation with very high-power short-duration lesions guided by left atrial wall thickness: the QDOT-by-LAWT randomized trial. Europace 2024;26(4):euae087.

Address for correspondence:

Minha Anees

Johann Radon Institute for Computational and Applied Mathematics (RICAM), Austrian Academy of Sciences (ÖAW)

Altenbergerstrasse 69, 4040 Linz, Austria

minha.anees@ricam.oeaw.ac.at